

# A Comprehensive Study of Lateral and Vertical Current Transport in Si/Si<sub>1-x</sub>Ge<sub>x</sub>/Si HBT's

Ž. Matutinović-Krstelj, V. Venkataraman, E.J. Prinz<sup>+</sup>, J.C. Sturm, and C.W. Magee\*

Princeton University, Dept. of Electrical Engineering, Princeton, N.J. 08544

<sup>+</sup> present address: APRDL, Motorola, Inc., Austin, TX 78721

\* Evans East, Plainsboro, N.J. 08536

## Abstract

We studied the effects of heavy doping and Ge concentration in the base on the dc performance of Si/Si<sub>1-x</sub>Ge<sub>x</sub>/Si npn HBT's. The lateral drift mobility of holes in heavily doped epitaxial SiGe bases is found to be lower than bulk Si values and independent of Ge content, and the Hall scattering factor is less than unity and decreases with increasing Ge concentration. For the vertical electron transport we have observed bandgap narrowing due to heavy base doping which is, to first order, independent of Ge concentration. Finally, a model for the collector current enhancement with respect to Si devices, including the effects of reduced density of states in the strained Si<sub>1-x</sub>Ge<sub>x</sub> base and the effective bandgap due to Ge and heavy doping, is presented.

## Introduction

In the recent years, Si/Si<sub>1-x</sub>Ge<sub>x</sub>/Si HBT's have received increasing attention and over 110GHz  $f_T$  has been reported [1]. To date, however, data for even dc modelling of these devices is particularly lacking, especially the effect of heavy base doping on vertical electron and lateral hole current. An important parameter in the design of HBT's for high-speed circuit applications is the base sheet resistance. To keep the sheet resistance low without increasing the base width, the base doping has to be increased. The reduction in gain due to heavier doping compared to Si BJT's is compensated by the bandgap offset between Si and Si<sub>1-x</sub>Ge<sub>x</sub>. Both the doping effects and the effects of Ge are important to understand and accurately predict the performance of Si/Si<sub>1-x</sub>Ge<sub>x</sub>/Si HBT's.

It is well known that the collector saturation current density of an HBT with flat Ge and doping profiles

in the base can be modeled as:

$$J_{co} = \frac{qD_n N_c N_v}{G_B} e^{-\frac{E_{Geff}}{k_B T}} \quad (1)$$

where  $D_n$  is the minority carrier diffusion coefficient,  $N_c$  and  $N_v$  are conduction and valence band densities of states,  $G_B$  is the Gummel number in the Si<sub>1-x</sub>Ge<sub>x</sub> base, and  $E_{Geff}$  is the effective bandgap for minority carrier concentration in the base. The effective bandgap is determined by the Ge concentration in Si<sub>1-x</sub>Ge<sub>x</sub>, but narrowing due to heavy doping, observed in Si [2] and SiGe [3], should also be taken into account. Since base sheet resistance is an important parameter in HBT design, and usually more often measured than the exact base Gummel number, by using the Einstein relation and  $R_s = (q\mu_p G_B)^{-1}$  we can rewrite (1) as:

$$J_{co} = qk_B T \frac{(N_c N_v)_{SiGe}}{(N_c N_v)_{Si}} n_{i0}^2 \mu_n \mu_p R_s e^{\frac{\Delta E_{Geff}}{k_B T}} \quad (2)$$

where  $\mu_p$  and  $\mu_n$  are the lateral hole and vertical electron mobilities in p<sup>+</sup>-base, respectively,  $n_{i0}^2$  is the intrinsic carrier concentration in Si and  $\Delta E_{Geff}$  is the bandgap reduction with respect to intrinsic Si. In this paper, we model the collector current by (2) using experimentally determined values for  $R_s$ ,  $\mu_p$ , and  $\Delta E_{Geff}$ , taking into account both Ge and heavy doping effects.

## Device Fabrication

We fabricated Si/Si<sub>1-x</sub>Ge<sub>x</sub>/Si HBT's with flat Ge and B profiles in the base grown by Rapid Thermal Chemical Vapor Deposition (RTCVD). Base dopings ranged from 10<sup>18</sup>cm<sup>-3</sup> to 10<sup>20</sup>cm<sup>-3</sup> and Ge concentrations ranged from 9% to 27%. Base widths varied from 300Å to 2000Å, depending on

the Ge concentration and all samples were strained. Undoped SiGe spacers were introduced to avoid parasitic barriers [4]. SIMS measurements confirmed flat profiles, base dopings and widths, and that the B-doping was contained within the SiGe layer (Fig. 1). Ge concentrations were confirmed by X-ray diffraction. Van der Pauw patterns for base resistance were made on each sample in addition to transistors. A simple double mesa wet-etch process without any thermal cycles over 400°C was used to prevent any possibility of parasitic barriers due to the thermal diffusion.

### Majority Carrier Properties

Fig. 2 shows Hall mobility of holes at room temperature as a function of base doping for different Ge concentrations ( $x$ ). For similar doping levels, Hall mobilities decrease with the increasing Ge concentration. By comparing the measured integrated hole concentration in the base by Hall measurements to those measured by SIMS we were able to relate Hall to drift mobilities and extract the Hall scattering factor. Fig. 3 shows Hall factor as a function of  $x$ . It is obvious that the Hall factor decreases with increasing Ge content and for  $x \geq 0.1$  is actually less than unity. Fig. 4 shows drift mobility as a function of base doping for different Ge concentrations. No strong dependence of drift mobility on Ge concentration was found. A simple fit to the data gives:

$$\mu_{p\text{drift}} = 20 + \frac{350}{1 + \left(\frac{N_A}{10^{17}\text{cm}^{-3}}\right)^{0.5}} \quad (3)$$

Temperature dependence of sheet resistivity was also measured on some samples and in the temperature range from 280K to 380K the values were within 15% of the room temperature value.

### Collector Current Measurements

Fig. 5 shows a typical Gummel plot of a transistor used in this study. The collector current is ideal over several orders of magnitude, and the negligible effect of the reverse collector bias indicates no parasitic barriers, even for very heavy dopings in the base ( $10^{20}\text{cm}^{-3}$ ), as confirmed by SIMS. Measurements on different area devices showed negligible perimeter effects.

We measured the temperature dependence of the collector current to extract the effective bandgap. Fig. 6 shows the activation energy  $E_A$  as a function of Ge concentration. The linear dependence on  $x$  is obvious and heavily doped devices seem to have slightly smaller bandgaps than the lightly doped ones for similar  $x$ . However, this method ignores the temperature dependence of minority carrier mobility which is known to be strongly dependent on temperature and doping [5,6] unlike the majority carrier mobility, especially at high doping levels. If the mobility varied by a factor of two from 280K to 380K this would cause an uncertainty of 65meV in the extracted  $E_A$ . Instead, the bandgap difference with respect to intrinsic Si was extracted from the room temperature data using (2). The SiGe density of states model of Prinz et al.[4] was assumed, and we used the Si model of Swirhun et al.[2] for electron mobilities as a function of B-doping, which is a reasonable approximation since we have observed no Ge dependence on hole drift mobilities at these doping levels. Fig. 7 shows the effective bandgap narrowing at room temperature as a function of Ge concentration for different doping levels. Fitting the data at the same doping level gives a bandgap offset with respect to Si of 7.32meV/1%Ge. We have subtracted the linear dependence on  $x$  and plotted the residual (apparent) bandgap narrowing vs. doping. This is shown in Fig. 8. The apparent bandgap narrowing clearly increases with increased doping and no Ge dependence was observed. Also shown in the figure are previously reported results by Swirhun et al.[2] and model by Klaassen et al.[7] for apparent bandgap narrowing in p-type Si. Although bandgap narrowing due to heavy doping is predicted (Jain et al.[8]) to be slightly higher in SiGe than in Si, and strain-dependent, our data shows lower values and a weaker doping dependence. The best fit to our data gives a total bandgap reduction (in meV) valid for  $N_A \geq 10^{18}\text{cm}^{-3}$ :

$$\Delta E_{G\text{eff}} = 44.0 + 13.6\ln\left(\frac{N_A}{10^{18}\text{cm}^{-3}}\right) + 732x \quad (4)$$

where  $N_A$  is the base doping and  $x$  the Ge concentration. Finally, Fig. 9 summarises the results. The relative collector current with respect to Si is plotted as a function of base sheet resistance for

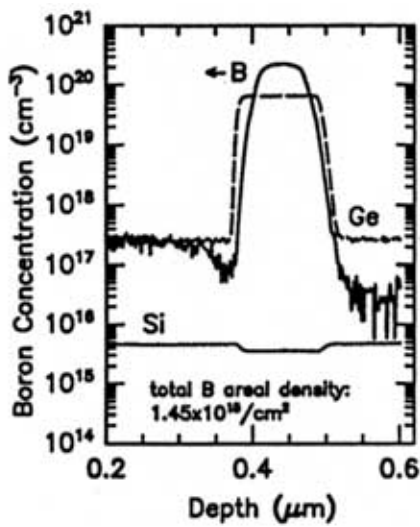


Figure 1: A typical SIMS profile of a device used in this study. Si and Ge are in arbitrary units. B was contained within the SiGe layer even for the heaviest doped devices.

various Ge concentrations. A relative collector current factor of one is defined for Si at the base sheet resistance of  $1\text{k}\Omega/\text{sq}$ . The lines are the model calculations assuming base widths of  $500\text{\AA}$ , drift mobilities given by (3), bandgap reduction by (4), strain-induced correction for densities of states given by [4] and electron mobility by [2]. Points show the data scaled to  $500\text{\AA}$  base-widths.

### Summary

Majority carrier properties in heavily doped strained  $\text{Si}_{1-x}\text{Ge}_x$  layers as well as collector currents of HBT's were characterized in the wide range of dopings and Ge concentrations for the first time. An empirical model for collector current including bandgap narrowing with respect to Si due to strain-dependent offset as well as heavy doping and strain-dependent densities of states is presented.

This work was funded by NSF and ONR.

### References

1. E. Crabbé et al, "113 GHz  $f_T$  graded-base SiGe HBT's," presented at the Dev. Res. Conf, Santa Barbara, CA, June 1993.
2. S.W. Swirhun, Y.-H. Kwark, and R.M. Swanson, "Measurement of electron lifetime, electron mobility, and bandgap narrowing in heavily doped p-type silicon," Tech. Dig. IEDM, p. 24 (1986).

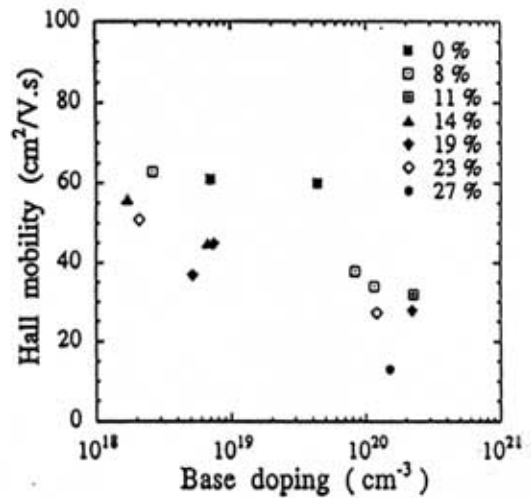


Figure 2: Hole lateral Hall mobility as a function of base doping for various Ge concentrations

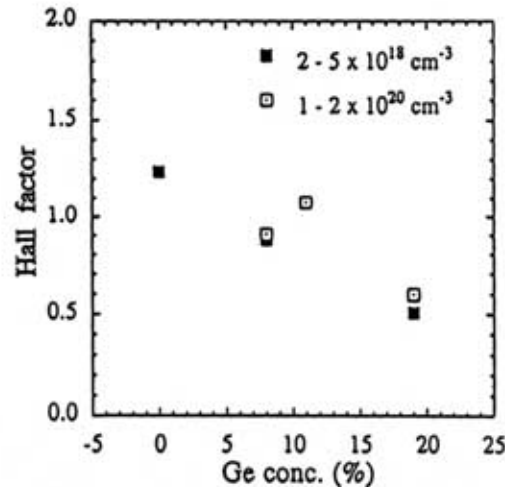


Figure 3: Hall scattering factor for holes as a function of Ge concentration

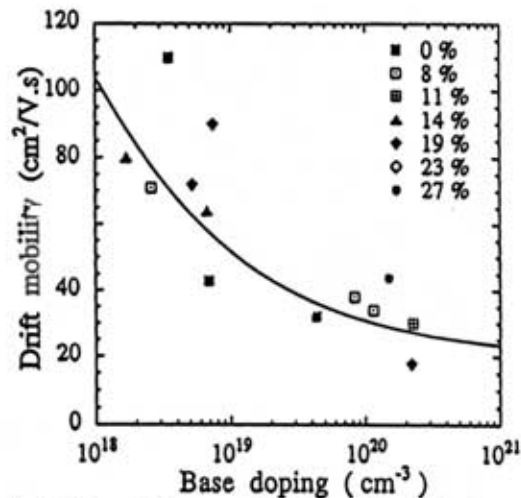


Figure 4: Drift mobility as a function of base doping. The line is the fit to data given by (3)

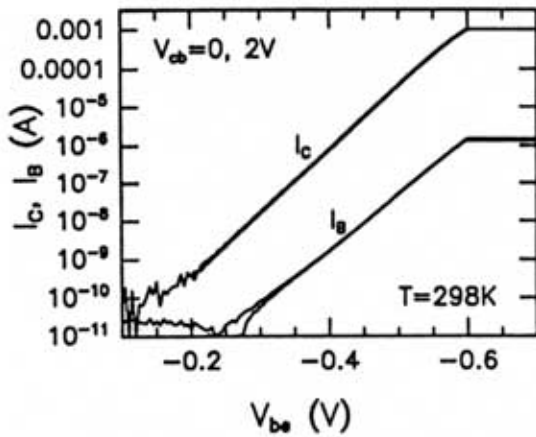


Figure 5: Typical Gummel plot of an HBT used in this study. Ge concentration in this device was 15% with the base doping of  $2 \times 10^{18} \text{ cm}^{-3}$

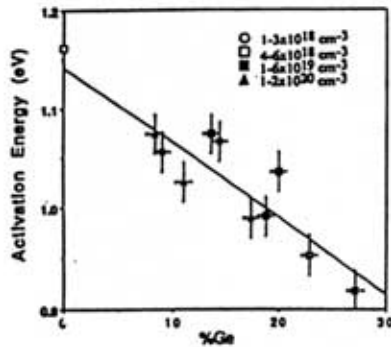


Figure 6: Activation Energy vs. Ge concentration for different base dopings.

3. J. Poortmans, S.C. Jain, et al, "Evidence of influence of heavy-doping induced bandgap narrowing on the collector current of strained SiGe-base HBT's," *Microelect. Eng'g* **19**, p. 443 (1992).
4. E.J. Prinz, P.M. Garone, P.V. Schwartz, X.Xiao, and J.C. Sturm, "The effect of base-emitter spacers and strain-dependent densities of states in Si/SiGe/Si HBT's," *Tech. Dig. IEDM*, p. 639 (1989).
5. S.E. Swirhun, D.E. Kane, and R.M. Swanson, "Temperature dependence of minority electron mobility and bandgap narrowing in  $p^+$  Si," *Tech. Dig. IEDM*, p. 298 (1988).
6. D.B.M. Klassen, "A unified mobility model for device simulation," *Tech. Dig. IEDM*, p. 357 (1990).
7. D.B.M. Klassen, J.W. Slotboom, and H.C. de Graaf, "Unified apparent bandgap narrowing in n- and p-type silicon," *Solid State Elect.* **35**, p. 125 (1992).
8. S.C. Jain and D.J. Roulston, "A simple expression for bandgap narrowing in heavily-doped Si, Ge, GaAs, and GeSi strained layers," *Solid State Elect.* **34**, p. 453 (1991).

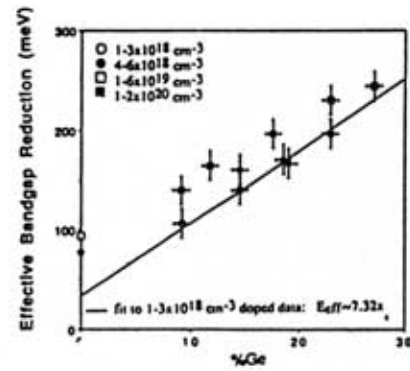


Figure 7: Total bandgap reduction with respect to intrinsic Si vs. Ge concentration

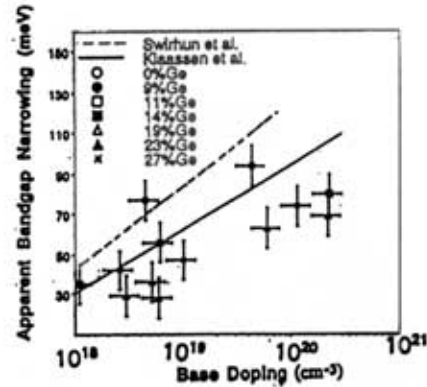


Figure 8: Apparent bandgap narrowing vs. base doping after linear dependence of the bandgap reduction on Ge content has been subtracted

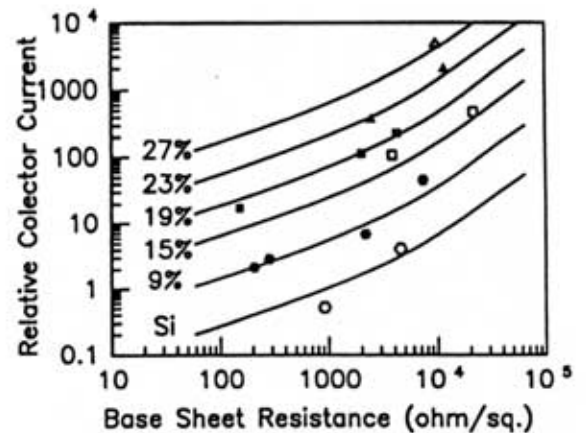


Figure 9: Relative collector current vs. base sheet resistance. The lines correspond to the model given by (2) with  $\Delta E_{Geff}$  of (4) and drift mobilities of (3). The points are the data